Deviation from Matthiessen's rule in electron-irradiated copper*

O. R. Alldredge, J. W. DeFord, and A. Sosin
University of Utah, Salt Lake City, Utah 84112
(Received 2 October 1974)

Deviations from Matthiessen's rule (which states that the electrical-resistivity contributions of two different types of scatterers in a metal are additive) occur generally. This paper concerns itself with the deviations arising from relatively simple scatterers: by point defects (vacancies and interstitials) created by electron irradiation and by phonons. Flexibility in the control of point-defect concentration is the major experimental feature of the work. Deviations from Matthiessen's rule in pure copper were studied over as wide a temperature range as possible, commensurate with the irradiation and annealing schedule used. In particular, the deviations were studied as effected by recovery in the first three major defect annealing stages. When analyzing effects due to stage-I annealing, damage was produced by irradiation at 4 °K; in stages II and III, damage was produced at 4 and at 80 °K. In all cases, the electron energy was 1.5 MeV. The deviations were analyzed by considering two deviation-producing mechanisms: the "two-band" model and changes in the temperature-dependent part of the electrical resistivity. At low temperatures (below 35 °K) the two-band form explains the data when separate temperature dependences for scattering of neck and belly electrons are taken into account. Contributions due to changes in the temperature-dependent part of the electrical resisitivity appeared to play no substantial part. In the stage-II region the deviations arising from irradiation at 4 °K and irradiation at 80 °K were of a similar form, indicating that the nature of the irradiation-induced scatterers in both cases were essentially the same. This may be explained by showing that the interstitials in either case existed as clusters—in the 80 °K case, nucleated on impurity traps and, in the 4 °K case, self-nucleated. In the stage-III region, contributions to the deviation from changes in the temperature-dependent part of the electrical resisitivity were quite large. Similarities between the deviations here and those arising in the neutron-irradiated copper without stage-III annealing give support to the model that the mobile defect in stage III is the vacancy.

I. INTRODUCTION

Electrical resistivity in metals is caused by scattering of conduction electrons by phonons, impurities, point defects, dislocations, grain boundaries, external surfaces, etc. If two different types of scatterers separately generate resistivities ρ_1 and ρ_2, then Mattheissen's Rule[1] (MR) states that the total resistivity $\rho(1,2)$ should be given by

$$\rho(1,2)=\rho_1+\rho_2. \tag{1}$$

MR may hold if the different scattering centers do not interact with one another, if the electrons are scattered elastically and isotropically, and if the Fermi surface is spherical. In general, these conditions are not met, giving rise to a deviation Δ from MR:

$$\Delta(1,2)\equiv\rho(1,2)-\rho_1-\rho_2. \tag{2}$$

Some main sources for deviations from MR are:

(i) Different anisotropies in the scattering behavior of the conduction electrons at different kinds of scatterers.

(ii) Interaction among the scattering centers. Interactions between phonons and static defects are of special importance. If the defects change the spectrum of lattice vibrations, they also change the phonon-induced resistivity. Also, the thermal excitation of the lattice vibrations might alter the effective scattering cross section of the defects, giving rise to a temperature dependence of the defect contribution to the electrical resistivity.

(iii) Inhomogeneities in the local distribution of the scattering centers in the sample over regions large compared to the mean free path of the electron. Such a situation would correspond to a partial shunting of the electron paths in the sample. The introduction of a second type of scatterer in random distribution removes this shunt and raises the resistivity contribution of the first type of scatterers.

There are a few other sources of deviations from MR discussed in the literature. These are electron-electron interaction and phonon drag,[2] alteration of the Fermi surface and of the effective number of conduction electrons by phonons or defects, and inelasticity of the electron scattering at phonons and defects.[3,4–6]

There have been many papers published about deviations from MR since the early investigations by Kohler[7] and by Sondheimer and Wilson.[3] Most of the experimental investigations reported have dealt with the temperature dependence of Δ in alloyed samples, or samples that have been irradiated or cold worked.[8–23] Until recently there has been a lack of any quantitative explanations of the phenomena, although there has been some qualita-

tive success with a "two-band" model.[15] Lately, Lengeler *et al.*[24] have published investigations studying deviations from MR in copper due to a variety of combinations of scatterers: gold impurities and phonons, nickel impurities and phonons, defects produced by cold work and phonons, defects produced by cold work, and point defects. Lengeler *et al.* report good quantitative agreement with theory using the two-band model among this host of scatterers.

Introducing defects through radiation damage provides an excellent way for studying deviations from MR. Most investigations of deviations from MR in alloys suffer from large sources of error caused by small errors in the geometrical factors of the samples studied. Radiation damage does not suffer from this problem since $\rho(T)$ can be measured for the same sample prior and subsequent to bombardment; the geometry of the sample remaining nearly constant. Electron irradiation is particularly attractive since it produces defects with much simpler structure than neutron damage or bombardment with positive ions. The doping (i.e., the fluence) is also easily varied by this method. A potential disadvantage, however, is a limitation to relatively low concentrations as compared to those produced by alloying.

Radiation damage in Cu anneals out[25] with increasing temperature in several well-defined stages. Stage I, occurring from 10 to 50 °K, is composed of a number of substages attributed to close-pair annihilation, correlated diffusion of interstitials to vacancies, and free migration of interstitials to more distant vancancies in the lattice and to other possible sinks or traps (e.g., impurities, dislocations, etc.). Approximately 85% of the damage anneals out in stage I in electron-bombarded Cu, less in neutron or positive-ion bombardment.

Stage II, occurring from 50 to about 250 °K, is much more gradual and is generally attributed to release of interstitials from impurity traps; the amount of annealing in this stage is found to be very dependent on the sample purity. Stage III occurs from approximately 250 to 330 °K, dependent on fluence (i.e., defect density). Its interpretation is a subject of controversy. Recovery is approximately 98% complete after stage III.

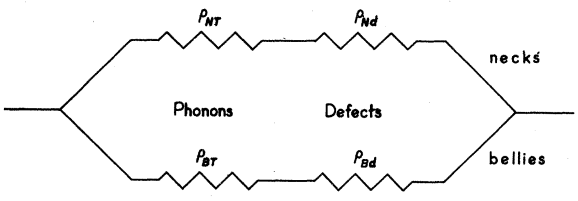

FIG. 1. Schematic representation of the two-band-model for the neck and belly electrons in copper containing phonons and defects as scatterers.

The following studies were preformed in this work:

(a) deviations from MR caused by phonons and defects introduced by radiation damage in the stage I region of Cu; (b) deviations from MR due to phonons and defects introduced by radiation damage produced at both 4 and 80 °K, followed by recovery in the stage II region of Cu; (c) deviations from MR caused by phonons and defects introduced by radiation damage produced at both 4 and 80 °K, followed by recovery in the stage III region of Cu.

II. THEORY

In the most detailed paper to date, that by Lengeler *et al.*,[24] the data are explained by considering two contributions to deviations from MR:

(i) deviations due to different anisotropies in the scattering behavior of the electrons at different scattering centers; (ii) deviations caused by the influence of the defects on the temperature-dependent part of the electrical resistivity. These two separate sources for deviation will be discussed and their additivity assumed: $\Delta = \Delta_1 + \Delta_2$.

A. Deviations due to different anisotropies in scattering behavior of conduction electrons

Sondheimer and Wilson[3] were the first to show that, if the conduction electrons in a metal exist in two distinct groups or bands, and even if MR is assumed to hold within each band, then deviations from MR exist. This gives rise to the two-band model. The two bands in Cu are associated with the anisotropy of the Fermi surface[26]: an almost spherical belly (band 1) with protrusions (necks) (band 2) in the ⟨111⟩ directions touching the Brillouin-zone boundary. The electrons in the region of the necks have mainly p-like character, while those in the vicinity of the bellies are s like. Hence, one would expect the belly electrons to have their greatest density at lattice sites while the neck electrons would move preferentially between the ion cores. Thus, a defect in a lattice site with a strongly localized potential would scatter mainly belly electrons; an interstitial-type defect would scatter mainly neck electrons. The total electrical conductivity σ is the sum of the conductivity due to each band so that the two bands may be considered as acting in the fashion of parallel resistors.

If consideration is now restricted to two particular scatterers, phonons and some other defect, and assuming MR holds in each band, the problem can be considered schematically as shown in Fig. 1.[15] Here the total phonon-induced resistivity ρ_T and the total resistivity due to defects ρ_d are given by

$$\rho_T = \rho_{NT}\rho_{BT}/(\rho_{NT}+\rho_{BT}) \text{ and}$$
$$\rho_d = \rho_{Nd}\rho_{Bd}/(\rho_{Nd}+\rho_{Bd}) . \quad (3)$$

In the simplest account of MR deviation, ρ_T is taken to be a function of temperature and ρ_d is taken independent of temperature. The deviation Δ, defined [as in Eq. (2)] by $\Delta = \rho(T) - \rho_T - \rho_d$, where $\rho(T)$ is the total resistivity at temperature T, can be shown to be given by

$$\Delta(T) = \frac{\alpha\beta\rho_T\rho_d}{\alpha\rho_T+\beta\rho_d} = \frac{(\gamma_T-\gamma_d)^2\rho_T\rho_d}{\gamma_d(1+\gamma_T)^2\rho_T+\gamma_T(1+\gamma_d)^2\rho_d} , \quad (4)$$

where

$$\gamma_T \equiv \rho_{BT}/\rho_{NT} = \sigma_{NT}/\sigma_{BT}, \quad \gamma_d \equiv \sigma_{Nd}/\sigma_{Bd} \quad (5)$$

are the ratios of the resistivities (or conductivities) in the neck and belly bands, and

$$\alpha = (\gamma_T-\gamma_d)^2/\gamma_T(1+\gamma_d)^2, \quad \beta = (\gamma_T-\gamma_d)^2/\gamma_d(1+\gamma_T)^2. \quad (6)$$

Note that this model assumes *no interband scattering* and that MR holds in each band. If a relaxation time can be defined for each point of the Fermi surface, the following relation holds[26]:

$$\gamma = \sigma_N/\sigma_B = S_N\nu_N\tau_N/S_B\nu_B\tau_B, \quad (7)$$

where S_N, ν_N, τ_N are the area, the mean Fermi velocity, and the mean relaxation time for the neck.[15] S_B, v_B, τ_B are the corresponding values for the belly band.

In the above equations, γ_d should reflect the scattering potential of the defect and thus should be essentially temperature independent. γ_T should be dependent on the phonon spectrum of the host lattice and thus would be expected to be temperature-dependent in the following manner. The relaxation time for belly electrons scattered by phonons increases with decreasing temperature because the average wave vector of the phonons decreases and umklapp processes die out. Thus the belly electrons suffer mainly only small-angle scatterings. For the neck electrons, the proximity of the Brillouin-zone boundaries prevents umklapp processes from dying out, even at very low temperatures. Therefore, the ratio τ_N/τ_B will be small at very low temperature. (We return to the actual temperature below.) In contrast, at high temperatures there are a large number of phonons with large wave vectors so the scattering will be almost the same for neck and belly electrons.

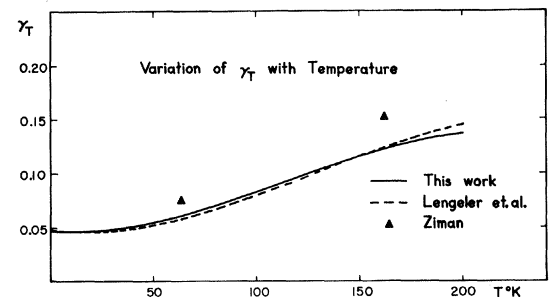

FIG. 2. Variation of $\gamma_T \equiv \sigma_{NT}/\sigma_{BT}$ (conductivity ratio for scattering of neck and belly electrons at phonons) for copper with temperature.

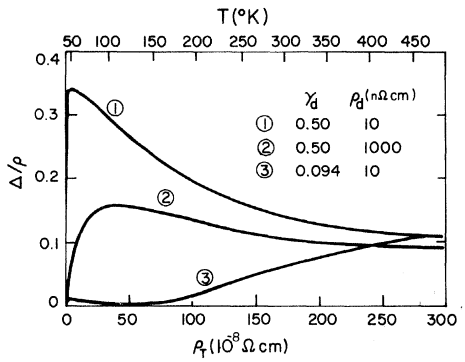

FIG. 3. Theoretical predictions of the two-band model for Δ/ρ_d as a function of ρ_T.

Lengeler *et al.* found the values for γ_T as a function of T shown by the dashed line in Fig. 2. Two values theoretically predicted by Ziman[27] are also plotted.

From Eq. (4) we have

$$\Delta/\rho_T = \alpha\beta\rho_d/(\alpha\rho_T+\beta\rho_d), \quad (8)$$

and for low T, $\rho_d \gg \rho_T$,

$$\Delta/\rho_T = \alpha. \quad (9)$$

Also, for high T, $\rho_T \gg \rho_d$,

$$\Delta/\rho_d = \beta = (\gamma_T-\gamma_d)^2/\gamma_d(1+\gamma_T)^2. \quad (10)$$

If γ_T is known, as from Lengeler *et al.*, Eq. (10) can be solved for γ_d. One obtains a quadratic equation giving two solutions for γ_d. In general, one finds one value of $\gamma_d > \gamma_T$ and one value for $\gamma_d < \gamma_T$. A theoretical prediction of Δ_1 as a function of ρ_T is shown in Fig. 3. The γ_T values used are those reported by Lengeler *et al.* Note the peak effect present in curve 1 which decreases with increasing dose as shown in curve 2. Note also that in curve 3, where $\gamma_d < \gamma_T$, the behavior of Δ/ρ_d as a function of ρ_T is dramatically different although the same saturation value, given by β, is obtained.

Some authors,[15,24] in explaining deviations from MR due to cold work and phonons, and neutron-radiation damage and phonons, have taken the case of γ_d less than γ_T to obtain values for γ_d. Yet their experimental observations indicate sharp rises in Δ/ρ_d towards a maximum with ρ_T, in contrast to curve 3. This choice of the solution for γ_d must be incorrect if the two-band model is to be credited as the major source of the deviations for MR.

Due to the cross section for electron-radiation damage of copper, irradiations for practical time intervals effectively limited this experiment to considering only the low-dose regions typified by curve 1 of Fig. 3. For example, consider a typical dose characterized by curve 2, 1000 $n\Omega$ cm. To produce this dose, after annealing above stage I, using a flux density of 10 $\mu A/cm^2$ (flux densities much larger than this produce excessive heating in the samples), a sample would have to be bombarded for ~8 months at 4 °K and it would require ~1000 years for the high-purity samples used in run II to reach this dose through 80 °K irradiation.

B. Deviations from MR caused by influence of defects on temperature-dependent part of electrical resistivity

A detailed investigation of this mechanism has been published by Kagan *et al.*[28] They find this deviation, Δ_2, by calculating transition probabilities in the first Born approximation using van Hove scattering correlation functions under the following assumptions: (a) the electrons are assumed free; (b) the defects do not alter the electron density of states; (c) only monatomic metals with cubic symmetry are considered; (d) nonmagnetic impurities or defects are statistically distributed in the lattice with a small concentration c; (e) oscillations of the real and perturbed lattice are considered in the harmonic approximation; (f) only zero- and one-phonon processes are considered; (g) the mass of an impurity $M_2 = M_1(1+\epsilon)$, where M_1 is the mass of the host atoms. Kagan *et al.* found that, in calculating the electrical resistivity from the derived scattering cross section, the inelastic incoherent cross section was the only important contributing part and obtained

$$\Delta_2 = 2c[\epsilon + (a_2 - a_1)/a_1]\rho_T, \quad 4\ ^\circ\mathrm{K} < T \ll \Theta \tag{11}$$

$$\Delta_2 = 2c[(a_2 - a_1)/a_1]\rho_T, \quad T \gtrsim \Theta \tag{12}$$

where Θ is the Debye temperature and a_2 and a_1 are the atomic form factors of the impurities and host-lattice atoms, respectively (it is assumed that the ions are well screened), and c is the concentration of the defects.

Lengeler *et al.* extended results of Kagan *et al.* to the possibility of changing coupling constants in the lattice and obtained

$$\Delta_2(T) = c(2\epsilon + 2\eta - 3\xi)\rho_T, \quad T \ll \Theta \tag{13}$$

$$\Delta_2(T) = c(2\eta - \xi)\rho_T, \quad T \gtrsim \Theta \tag{14}$$

where $\epsilon = (M_2 - M_1)/M_1$ and $\eta = (a_2 - a_1)/a_1$. It is easily seen that, depending on the sign of η and ξ (and their relative magnitudes), $\Delta_2(T)$ can be either positive or negative. This is in contrast to Δ_1, which must always be positive. Considering only Δ_1 and Δ_2, it therefore follows that all deviations from MR must be positive except for those due to changes in the temperature-dependent part of the electrical resistivity.

Note that $\Delta_2(T)$ may be looked upon as a perturbation solely on ρ_T. With Δ_1 and Δ_2 calculated from the above models, the two contributions may be separated from one another by noting that for $T \ll \Theta$,

$$\Delta_1(T) = \alpha\rho_T \tag{15}$$

and

$$\Delta_2(T) = c(2\epsilon + 2\eta - 3\xi)\rho_T, \ c = \rho_d/\rho_f, \tag{16}$$

where ρ_f is the contribution of Frenkel pairs to the electrical resistivity. If it is assumed, as found by Lengeler *et al.*, that neither γ_d nor γ_T are functions of ρ_T or ρ_d at low T, then the slope of a plot of Δ versus ρ_T at low T should be constant α for Δ_1, independent of ρ_d. For Δ_2, however, this slope should be proportional to defect concentration or dose ρ_d. These predictions were, in fact, observed by Lengeler *et al.* in their work with gold and nickel impurities in copper.

III. EXPERIMENTAL

A. Apparatus

Resistance was determined in the experiment by measuring potential difference for a known current. In order to convert to resistivity, the geometry factor F, defined by $F = L/A$, must be known for the sample in question. Here L is the length of the sample and A is the cross-sectional area. Thus resistance $R = F\rho$. A major advantage of electron bombardment in investigating deviations from MR is that $\rho(T)$ can be measured for the same sample before and after irradiation. Thus in all determinations of quantities, such as Δ/ρ_d, the geometry factor cancels out. It is therefore sufficient to determine the geometry factor from the resistance of the sample at room temperature; this will give an absolute accuracy of 2 or 3%, which is sufficient for the purpose of determining ρ_T.

Two separate runs were made. The sample for run I was obtained from Coltmann, Oak Ridge National Laboratory, and was 99.999%, multipass zone-refined copper. The samples were subsequently drawn to 0.0056 in., etched, and then annealed in quartz tubing while suspended from quartz supports at 1000 °C for 2 h in an atmosphere of 5×10^{-4}-Torr air. This "internal-oxidation treatment" produced samples with a resistance ratio of

$$\rho_{295\,^\circ\mathrm{K}}/\rho_{4\,^\circ\mathrm{K}} = 2300 \text{ or } \rho_0 = 0.73\ n\Omega\,\mathrm{cm}\ (4\ ^\circ\mathrm{K}).$$

The samples used in run II were American Smelting and Refining Co. 99.999% pure copper, drawn to 0.0056 in., etched, and then annealed. The annealing treatment here was also performed in a quartz tube at 1000 °C for 2 h in 5×10^{-4}-Torr

air, but here the samples were suspended from graphite supports. This treatment typically gave a ratio of about 2000+, about equivalent to run I. However, 80 °K damage-rate experiments showed damage rates much less than in run I implying a *lower* effective impurity-trap concentration in the sample of run II; see below.

At 80 °K, a free interstitial produced by irradiation is very mobile and has a very short lifetime before reacting with an impurity or vacancy or another interstitial already trapped by an impurity. Consequently, during irradiation the instantaneous concentration of interstitials in the lattice is very low, giving an extremely low probability for the formation of stable diinterstitial or higher interstitial clusters (consisting solely of interstitials, not impurities). Thus, the 80 °K damage rate should bear a direct relationship to the concentration of impurity traps.

To effect good thermal conductivity, the samples were mounted on sapphire insulators, using the technique described by Sosin and Neely.[29] The current and potential leads were soft-soldered to the sample.

For the irradiation and measurement of resistivity at various temperatures, a liquid-helium cryostat was used, similar to that described by Sosin and Neely.[29] The main feature of this arrangement was a sample holder connected by means of a thin-wall stainless-steel tube through a valve to the liquid-helium reservoir. By opening or closing the valve, the samples could be either subjected to or isolated from liquid-helium environment. A 45-Ω heating coil at the end of the tube was used to heat the samples. Any temperature from 4 to 370 °K was easily attainable. Temperature was measured by means of a Cu vs Au–2.1-at.%-Co thermocouple. This proved insensitive to radiation damage and was reproducible over the entire temperature range to within 0.5%. Reproducibility to within 0.002 °K was obtained by means of a dummy sample, originally calibrated by this thermocouple.

Temperature control was by means of a negative feedback system; control to within ± 0.005 °K or better was attainable over the temperature range of 4 to 250 °K.

A 2-MeV Van de Graaff accelerator was used as the irradiation source. The flux was measured using a standard Faraday cage and passing the beam through a slit system of known area. The Faraday cage was connected to an Elcor current integrator. In order to ensure homogeneous damage over the sample, the beam was swept vertically at about 3300 Hz and horizontally at 150 Hz.

Potential measurements were made using a Honeywell Rubicon model 2768 six-dial potentiometer with a Leeds and Northrup nanovolt 9838-1 detector. This system allowed measurements to be made to within 10 NV. To eliminate thermal emf's, potential measurements were made with the currents reversed. In the determination of Δ, Δ is calculated from four separate measurements, each with a maximum uncertainty of 0.01 μV, giving a maximum uncertainty of 0.04 μV.

Because of the relatively short length of samples suitable for these measurements, it was necessary to measure changes in potential of one part in 10^5. This was achieved by balancing the dummy sample against the irradiated sample and measuring the differences between them at various radiation doses and temperatures. The limiting factor in the experiment then became the stability of the constant-current power supplies. These were Hewlett-Packard model 6177B supplies and proved stable to about one part in 10^5.

It should be noted that the two above-mentioned major contributors to experimental uncertainty are independent of the radiation-induced defect concentration, while Δ is approximately proportional to defect concentration. The percentage error in Δ thus decreases as the defect concentration is increased. In most cases the uncertainty in the data displayed in the figures is smaller than or of the order of the size of the data points. Marked exceptions to this occur in the curves found from the lowest radiation-induced defect concentrations. In these cases, the scatter in data points indicates the precision of the measurements.

B. Experimental results

Figures 4 and 5 show the damage production at 80 °K in samples I and II, respectively, as a function of electron fluence.

In run I, the sample was bombarded at 80 °K then annealed at 230 °K, and $\Delta(T)$ was found as a function of temperature up to 220 °K. The sample was then annealed at 260 °K and $\Delta(T)$ was again examined. The results are shown in Fig. 6.

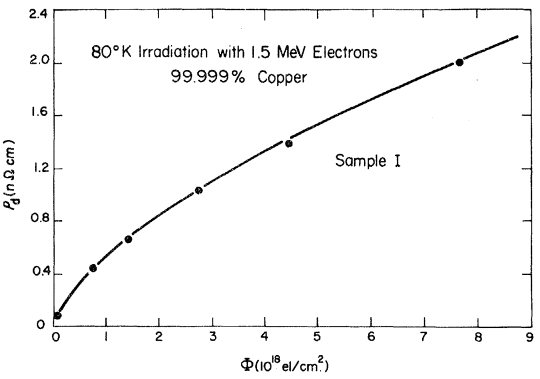

FIG. 4. Damage production at 80 °K as a function of electron fluence.

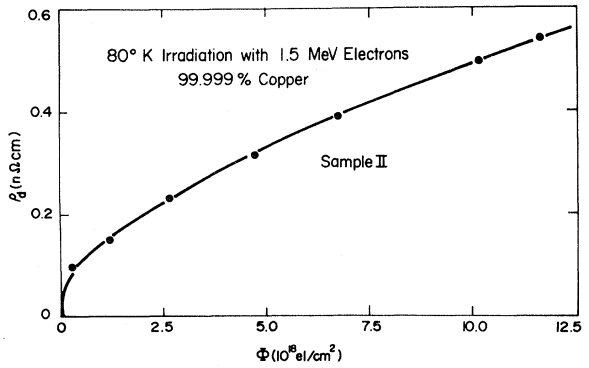

FIG. 5. Damage production at 80 °K as a function of electron fluence.

In run II, the sample was bombarded at 80 °K and then annealed at 220 °K and $\Delta(T)$ found. It is interesting to note that almost no annealing occurred between 80 and 200 °K. This was performed three times, following progessively increasing electron doses. The results are shown in Fig. 7. This sample was then annealed at 370 °K to remove as much damage as possible; 0.29 nΩcm of damage was left after this anneal. Then the sample was bombarded at 4 °K, then annealed at 200 °K, and $\Delta(T)$ was found. This was done four times, giving four progressively increasing doses. The results are shown in Fig. 8. Figure 9 shows the results when the damage produced at 4 °K in run II and the damage produced at 80 °K in run I was annealed through stage III.

Finally, after the damage produced in run I was annealed through stage III, an anneal was performed at 370 °K to remove as much damage as possible; 0.10 nΩcm was left after this anneal. The sample was then bombarded at 4 °K and anneals were performed through stage I, determining $\Delta(T)$ after each anneal. The results are shown in Fig. 10.

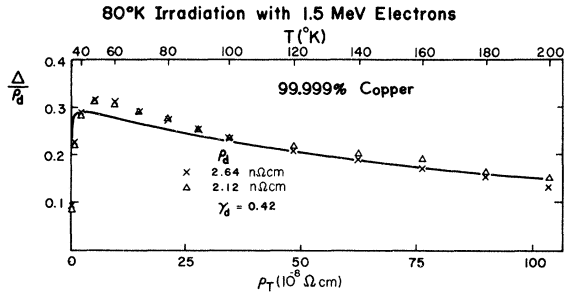

FIG. 6. Relative deviation from MR, Δ/ρ_d, versus ρ_T in sample I. The sample was irradiated at 80 °K, warmed from 4 to 230 °K (×'s), cooled, then warmed a second time (△'s). The solid line shows a theoretical fit to the data given by the two-band model.

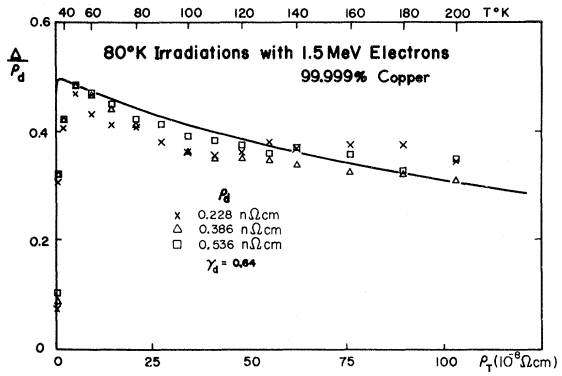

FIG. 7. Relative deviation from MR, Δ/ρ_d, versus ρ_T in sample II. The sample was irradiated at 80 °K, then warmed from 4 to 220 °K (×'s), reirradiated at 80 °K, warmed from 4 to 220 °K again (△'s), and repeated a third time (□'s). The solid line shows a theoretical fit to the data given by the two-band model.

IV. DISCUSSION

A. Effects of stage II annealing

Using equations of Sec. II, γ_d and γ_T were found as functions of temperature in a self-consistent manner, using the values of γ_T obtained by Lengeler *et al.* as first approximations to γ_T. The values of γ_d obtained were independent of temperature and are shown in Figs. 6–8. The results for γ_T are shown in Fig. 2. Final agreement between Lengeler and the present work was good. In Figs. 6–8 the solid lines show a theoretical fit, using the two-band model, to the data. It should be noted that in Fig. 7 the large scatter in the points is due to the small-defect concentrations attainable during the 80 °K bombardment in run II, because of the extremely low damage rate for this sample.

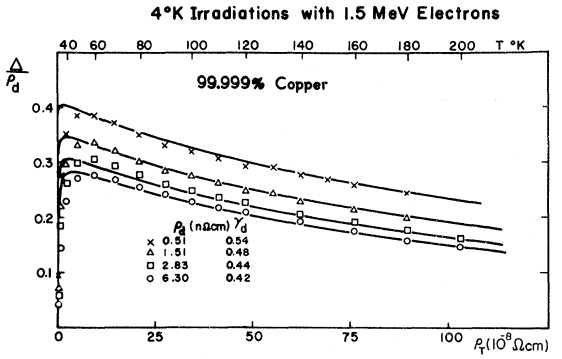

FIG. 8. Relative deviation from MR, Δ/ρ_d, versus ρ_T in sample II (copper) irradiated at 4 °K and subsequently annealed at 220 °K. Then $\Delta(T)$ was measured. This entire procedure was gone through four times, yielding higher ρ_d values in each measurement set. The solid lines show theoretical fits to the data given by the two-band model.

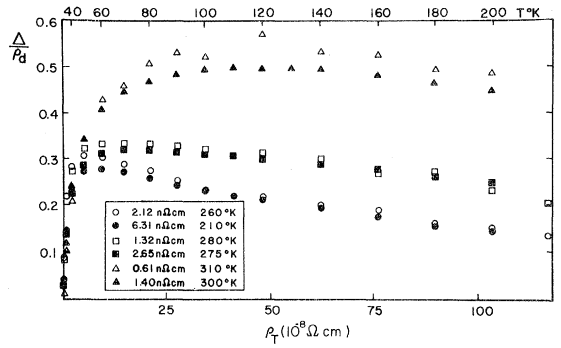

FIG. 9. Relative deviation from MR, Δ/ρ_d, versus ρ_T when sample I irradiated at 80 °K (open points) and sample II irradiated at 4 °K (filled points) are annealed through state III. The defect concentration ρ_d remaining after annealing and the annealing temperature are also shown.

For the doses achieved in this experiment, the two-band model predicts that, if γ_d is a constant independent of dose, Δ/ρ_d will be a function of temperature only and not of dose for $\rho_T \gg \rho_d$; see Eq. (10). This seems to be true in Figs. 6 and 7.

In Fig. 8 the progression of curves can be correlated by noting that γ_d decreases with increasing defect concentration (ρ_d). The shape of the curves in Fig. 8 and in Figs. 6 and 7 are quite similar, although Fig. 8 was produced by irradiating at 4 °K. This might at first seem surprising since one might expect the defect configuration resulting from an irradiation at 4 °K and subsequent annealing above stage I to be quite different than that produced by irradiation at 80 °K. However, the analysis of Waite,[30] as extended by Simpson and Sosin[31] and by Thompson *et al.*,[32] provides an explanation in terms of the effective trap concentrations for the samples deduced from the damage rate at 80 °K. This theory gives for sample I, shown in Fig. 6, an effective trap concentration (for mobile interstitials) of about 1 ppm. For sample II, shown in Fig. 7, an effective trap concentration of 0.03 ppm was obtained. This implies an average number of interstitials per trap for Fig. 6 of about 11 and for Fig. 7 or approximately 30—70, depending on defect concentration. The

TABLE I. Values of α and β at particular temperatures.

T(°K)	α	β
15	1.12 ± 0.11	0.023 ± 0.003
20	1.30 ± 0.04	0.055 ± 0.001
25	1.17 ± 0.04	0.118 ± 0.005
30	1.07 ± 0.03	0.173 ± 0.003
35	1.11 ± 0.02	0.213 ± 0.002

TABLE II. Values for γ_T and γ_d at particular temperatures.

T(°K)	γ_T	γ_d
15	4.71×10^{-4}	0.024 ± 0.003
20	2.30×10^{-3}	0.060 ± 0.001
25	0.0114 ± 0.0014	0.142 ± 0.008
30	0.026 ± 0.002	0.231 ± 0.007
35	0.0365 ± 0.0015	0.297 ± 0.005

size of these numbers may seem surprising. However, Becker *et al.*[33] have obtained numbers for the average number of interstitials per trap for high-purity copper of a similar magnitude. Also, Shimomura[34] reports observing interstitial clusters, in 80 °K electron-irradiated gold before stage III annealing, of size up to about 10 Å in diameter. It seems clear that the interstitials produced by 80 °K irradiations exist strongly clustered on impurity traps.

The above theory applied to 4 °K irradiations gives that, for the lowest dose shown in Fig. 8, greater than 95% of the interstitials which survive stage I recovery exist as diinterstitials or high-order interstitial clusters. Schroder,[35] using the rate theory of Waite,[30] has been able to give estimates for the interstitial cluster size distribution, depending somewhat on the trapping radii of the various interstitial clusters. He obtained for the average cluster size 2.7–3.2, depending on the dependence of the cluster trapping radius on the number of interstitials in the cluster. This re-

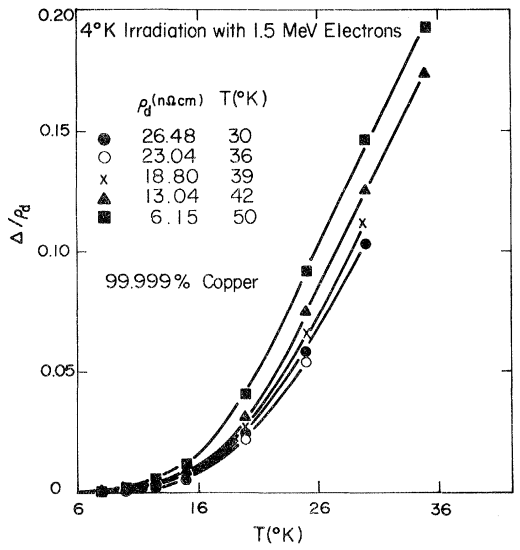

FIG. 10. Relative deviation from MR, Δ/ρ_d, versus temperature in sample I irradiated at 4 °K and then annealed through stage I. The defect concentration ρ_d remaining after annealing and the annealing temperature are also shown.

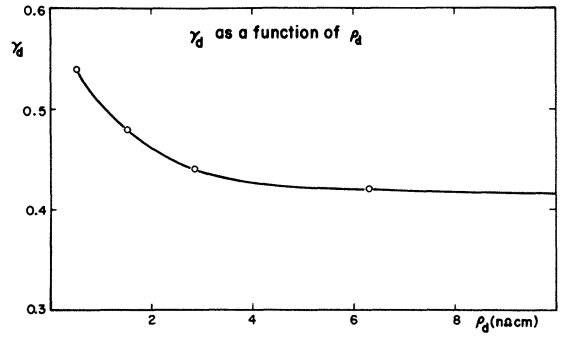

FIG. 11. Variation of $\gamma_d \equiv \sigma_{Nd}/\sigma_{Bd}$ (conductivity ratio for scattering of neck and belly electrons at defects) with defect concentration produced by irradiation with 1.5-MeV electrons at 4 °K and subsequently annealed at 220 °K.

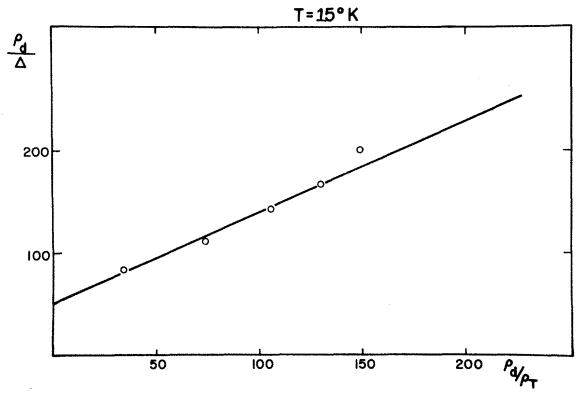

FIG. 13. Variation of ρ_d/Δ with ρ_d/ρ_T at constant T = 15 °K for sample I irradiated at 4 °K and subsequently annealed in stage I.

sult is independent of defect concentration, assuming one starts with an unirradiated sample. Unfortunately, in the 4 °K irradiations shown in Fig. 8, each succeeding dose had the preceding residual damage as its initial damage condition. This will result in varying initial conditions, resulting in a progressively increasing average cluster size, as the defect concentration is increased in the above manner. It is reasonable to assume that this increase in the relative proportion of higher-order interstitial clusters with increasing dose causes a change in the average anisotropy for an interstitial cluster with respect to scattering of the neck and belly conduction electrons, thus giving rise to a changing γ_d. γ_d, plotted as a function of dose produced at 4 °K, is shown in Fig. 11. It can be seen that γ_d tends to approach a saturation value of about 0.42 as $\rho_d \to \infty$. If the interstitial clusters nucleated on traps scatter similarly, similar results should be obtained. Indeed, the saturation result of $\gamma_d = 0.42$ in Fig. 11 is just the value obtained for γ_d in Fig. 6. Furthermore, since $\gamma_d \propto \tau_N/\tau_B$, the decrease of γ_d as ρ_d increases implies, in terms of the two-band model, that higher-order interstitial clusters tend to scatter neck electrons more strongly than do simple di-interstitials.

Next consider the similarities and differences between the results produced by bombardment at 4 °K and 80 °K. In all cases the two-band model gives a reasonable fit to the data for ρ_T greater than about 20×10^{-8} Ω cm (65 °K). The main difference between the 4 and 80 °K bombardments appears to be a shift in the position of the peak from 50 °K ($\rho_T = 50$ nΩ cm) in the 80 °K bombardments to 60 °K ($\rho_T = 90$ nΩ cm) for the 4 °K bombardments.

A more detailed examination of the region below about 65 °K than is shown in Figs. 6–8 reveals that the two-band model gives a theoretical prediction for Δ/ρ_d (using values of γ_d and γ_T found appropriate for the higher-temperature regions) significantly larger than found by experiment. In fact, a close examination of the data of Lengeler *et al.*, in their alloy work at low temperatures, show a similar effect. They attribute this to interference from the residual impurities present before doping or irradiation. However, they found this effect quite significant even up to defect levels over 100 times greater than the residual impurity levels. The two-band model predicts that at low T, $\Delta = \alpha\rho_T$, independent of dose. However, the data in Fig. 6 (80 °K irradiations using sample I) show that, at constant ρ_T and very low T, Δ is proportional to ρ_d. These results are displayed in Fig. 12. For deviations from MR caused by changes in the temperature-dependent part of the electrical resistivity, Eq. (16) shows that Δ_2 = (const.) $\rho_T\rho_d$. Figures 12 shows that Δ is proportional to ρ_d but does not vary linearly with ρ_T until $\rho_T \gtrsim 0.80$ nΩ cm. Perhaps the residual impurities are interfering here. Unfortunately, because of experimental problems, measurement at these low values of ρ_T could not be made in run II, displayed in Figs. 7 and 8. What data there are

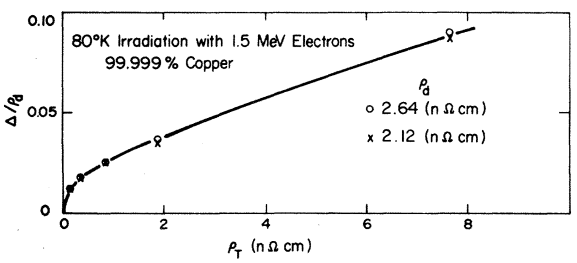

FIG. 12. Relative deviations from MR, Δ/ρ_d, versus ρ_T due to phonons in sample I irradiated at 80 °K and subsequently annealed at 220 °K. The low ρ_T region is shown.

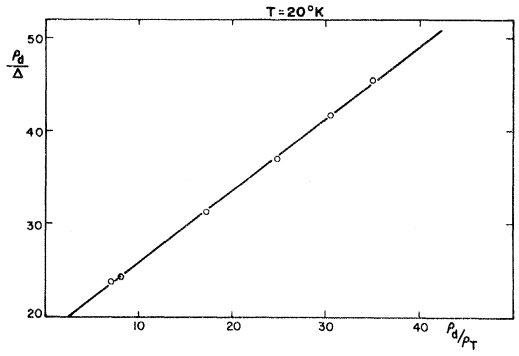

FIG. 14. Variation of ρ_d/Δ with ρ_d/ρ_T at constant T = 20 °K for sample I irradiated at 4 °K and subsequently annealed in stage I.

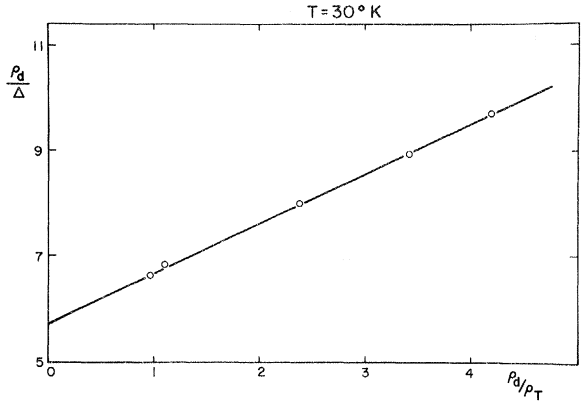

FIG. 16. Variation of ρ_d/Δ with ρ_d/ρ_T at constant T = 30 °K for sample I irradiated at 4 °K and subsequently annealed in stage I.

tend to indicate, however, that changes in the temperature-dependent part of the electrical resistivity are, at least at low ρ_T, a significant contribution to the deviation from MR.

Finally, one is struck by the similarities between Figs. 6–8 and other authors' [15,16,18,24] results for doped metals. Also, the results for γ_d of 0.4–0.5 for this experiment are very similar to the results of Lengeler *et al.* for gold and nickel impurities in copper ($\gamma_d = 0.50$ for Au; $\gamma_d = 0.44$ for Ni).

Assuming with Lengeler *et al.* that single interstitials are preferential scatterers of p-type or neck electrons and vacancies are preferential scatterers of s-type or belly electrons and that equal numbers of interstitials and vacancies are produced in the lattice by electron irradiation, one might expect $\tau_N/\tau_B \simeq 1$ for this experiment, considering only defect-scattering relaxation processes. In the two-band model, $\gamma_d \simeq \frac{1}{6}\tau_N/\tau_B$; this would result in $\gamma_d \simeq 0.16$. However, if it is assumed that interstitial *clusters*, because of their increased size, scatter neck and belly electrons about equally, one would expect a preponderance of belly electron scattering, largely by vacancies, resulting in $\tau_N/\tau_B > 1$. Values of γ_d of about 0.5 would then not be unreasonable.

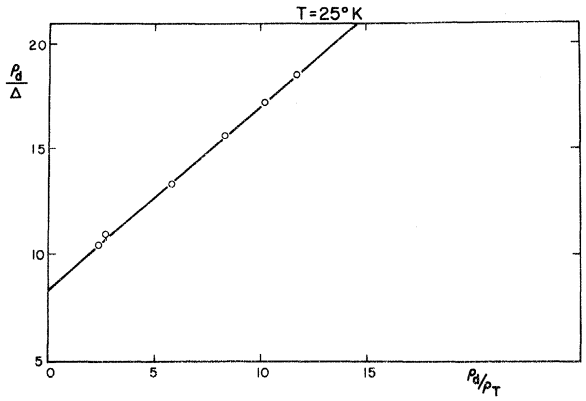

FIG. 15. Variation of ρ_d/Δ with ρ_d/ρ_T at constant T = 25 °K for sample I irradiated at 4 °K and subsequently annealed in Stage I.

B. Effects of stage III annealing

In Fig. 9 a similar behavior is exhibited by both the sample bombarded at 4 °K and the sample bombarded at 80 °K. In both cases, the curve showing Δ/ρ_d as a function of ρ_T obtained by annealing below the onset of stage III changes dramatically as the damage is annealed out through stage III. As the samples are annealed, the maxima in the curves shift to higher T and become larger. Instead of the high-temperature part of the curve following the two-band model, the curves fall off less rapidly with temperature at first and decrease in a quasilinear manner with ρ_T. These curves cannot be explained in any direct manner by the two-band model. The rise in the maxima could be explained by γ_d becoming larger, but not the shift in position of the maxima towards higher ρ_T. The two-band model predicts that, as defect concentration becomes less, the maxima should shift to *lower* ρ_T, the opposite of what is observed. Further, the behavior of Δ/ρ_d, when ρ_T is large, is governed by changes in γ_T with ρ_T. Since γ_T is a characteristic quantity of the host lattice for the two-band model, it should not change its behavior upon annealing. Yet upon annealing the curves no longer decrease as before with increasing ρ_T; instead they begin to decrease quasilinearly with a slope that decreases as higher annealing temperatures are attained.

The progression of the curves shown in Fig. 9. does not correlate with defect concentration, but appears to correlate well with annealing temperature. As the annealing temperature increases,

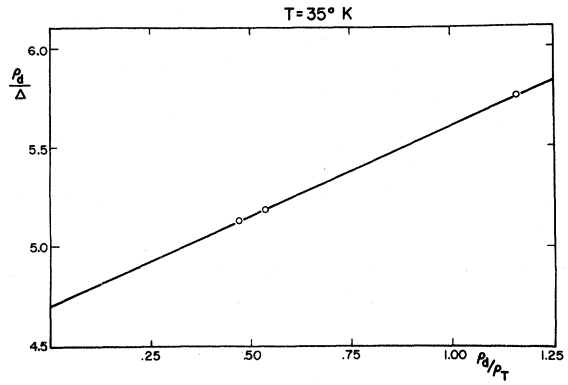

FIG. 17. Variation of ρ_d/Δ with ρ_d/ρ_T at constant T = 35 °K for sample I irradiated at 4 °K and subsequently annealed in stage I.

each curve reaches a higher maximum and becomes flatter. *The bombardment temperature seems to play no part.* Lengeler *et al.* report similar behavior for neutron-irradiated copper. However, they find this behavior even at annealing temperatures well *below* stage III.

In contrast to the isolated Frenkel pairs produced by electron[25] damage, fast neutron irradiation produced highly energetic recoil atoms which initiate large displacement cascades leading to the survival of clusters of interstitials and vacancies. In this experiment's electron-irradiated samples, the interstitial atoms already exist in clusters, while the vacancies are distributed singly and randomly in the lattice, when a sample is annealed below stage III. Thus, one difference in defect configuration between electron-irradiated samples annealed below stage III and neutron-irradiated samples are the vacancy clusters which are present in the neutron-irradiated sample. Since the shape of the curves for deviations from MR should characterize the defect configurations, the similarity between the curves for neutron irradiation and electron irradiation annealed in the stage III region could reflect the build-up of vacancy clusters in the stage III region of copper.

Currently, there are two major theories of the annealing in stage III for copper[25]:

(i) Vacancy model—In this model, stage III is attributed to the migration of single vacancies which recombine with the trapped and clustered interstitials remaining after stage I, and which cluster with other vacancies.

(ii) Conversion-two-interstitial model—The basic idea of the conversion-two-interstitial model is the assumption of a metastable configuration in which interstitials can migrate freely in stage I with the alternative possibility for conversion of these interstitials into a more stable configuration, particularly at higher temperatures. This second configuration is thought to be immobile up to the temperature of stage III, where it can migrate freely by thermal activation.

The results of this experiment tend to support vacancy migration, if vacancy clusters are the primary consideration in the character of Fig. 9.

As has been mentioned, at high ρ_T, Δ/ρ_d decreases linearly with ρ_T. From Eq. (14), Δ/ρ_d is const. $\times\rho_T$, where this constant may be positive or negative, depending on the relative sizes of η and ξ. Thus, this linear decrease with ρ_T is as predicted, indicating that a significant portion of the deviation from MR in the stage III region is due to Δ_2 arising from changes in the temperature-dependent part of the electrical resistivity.

C. Effects of stage I annealing

Figure 10 displays results obtained by measuring the deviation from MR in the stage I region of copper and in this form does not appear to be too illuminating. However, Eq. (4), rearranged, is

$$\rho_d/\Delta = 1/\beta + (1/\alpha)(\rho_d/\rho_T), \tag{17}$$

where α, β may be functions of temperature but not of dose. Thus, if ρ_d/Δ is plotted vs ρ_d/ρ_T at a constant temperature, a straight line should be obtained. Curves obtained in this manner are displayed in Figs. 13–17 for T = (15–35) °K. In all cases, rms straight lines are plotted as the solid line and fit the data extremely well.

---

*Work supported by the U. S. Atomic Energy Commission under Grant No. At (11-1)1800. It is based in part on a dissertation submitted by O. R. Alldredge in partial fulfillment of the requirements for the Ph. D. degree.

[1]A. Matthiessen, Ann. Phys. Chem. 110, 190 (1960).
[2]R. P. Huebener, Phys. Rev. 146, 503 (1966).
[3]E. H. Sondheimer and A. H. Wilson, Proc. R. Soc. Lond. 190, 435 (1947).
[4]S. Koshino, Prog. Theor. Phys. 24, 484, 1049 (1960).
[5]P. G. Klemens, J. Phys. Soc. Jpn. Suppl. II 18, 77 (1963).
[6]P. L. Taylor, Proc. Phys. Soc. Lond. 80, 755 (1962); Phys. Rev. A 135, 1333 (1964).
[7]M. Kohler, Z. Phys. 126, 495 (1949).
[8]H. Wenzl, Habilitationsarbeit (Technische Hochschule Munich, 1966) (unpublished).
[9]E. Krautz and H. Schultz, Abh. Braunschweig. Wiss. Ges. 8, 55 (1956); Z. Naturforsch. A 12, 710 (1957).
[10]H. Schultz, Z. Angew. Phys. 9, 465 (1957).
[11]P. Alley and B. Serin, Phys. Rev. 116, 334 (1959).
[12]P. G. Klemens and G. C. Loewenthal, Aust. J. Phys. 14, 352 (1961).
[13]D. H. Damon and P. G. Klemens, Phys. Rev. 138, A1390 (1965).
[14]T. Farrell and D. Greig, Phys. Lett. A 24, 401 (1967).
[15]J. S. Dugdale and Z. S. Basinski, Phys. Rev. 157, 552 (1967).
[16]R. G. Stewart and R. P. Huebener, Phys. Rev. B 1,

3323 (1970).
[17]F. T. Hedgcock and W. B. Muir, Phys. Rev. 136, A561 (1964).
[18]K. B. Das and A. N. Gerritsen, J. Appl. Phys. 33, 3301 (1962).
[19]R. L. Powell, H. M. Roder, and W. J. Hall, Phys. Rev. 115, 314 (1959).
[20]H. Kreuzer, Diplomarbeit (Technische Hochschule, Munich, 1966) (unpublished).
[21]E. Krautz and H. Schultz, Z. Naturforsch. A 9, 125 (1954).
[22]J. W. Rutter and J. Reeckie, Phys. Rev. 78, 70 (1950).
[23]D. Bowen and G. W. Rodeback, Acta Metall. 1, 649 (1953).
[24]B. Lengeler, W. Schilling, and H. Wenzl, J. Low Temp. Phys. 2, 59 (1970); J. Low Temp. Phys. 2, 237 (1970).
[25]W. Schilling, G. Burger, K. Isebeck, and H. Wenzl, in *Vacancies and Interstitials in Metals*, edited by A. Seeger, D. Schumacher, W. Schilling and J. Diehl (North-Holland, Amsterdam, 1970), p. 255.
[26]J. M. Ziman, *Principals of The Theory of Solids* (Cambridge U. P., Press, 1965), p. 183.
[27]J. M. Ziman, Phys. Rev. 121, 1320 (1961).
[28]Y. Kagan and A. P. Zhernov, Zh. Eksp. Teor. Fiz. 50, 1107 (1966) [Sov. Phys. - JETP 23, 737 (1966)].
[29]A. Sosin and H. H. Neely, Rev. Sci. Instrum. 32, 922 (1961).
[30]T. R. Waite, Phys. Rev. 107, 463 (1957).
[31]H. M. Simpson and A. Sosin, Radiat. Eff. 3, 1 (1970).
[32]L. Thompson, G. Youngblood, and A. Sosin, Radiat. Eff. 20, 111 (1973).
[33]D. E. Becker, F. Dworschak, and H. Wollenberger, Phys. Status Solidi 47, 171 (1971).
[34]Y. Shimomura, Philos. Mag. 19, 773 (1969).
[35]K. Schroder, thesis (Technische Hochschule, Aachen, Germany, 1969) (unpublished).